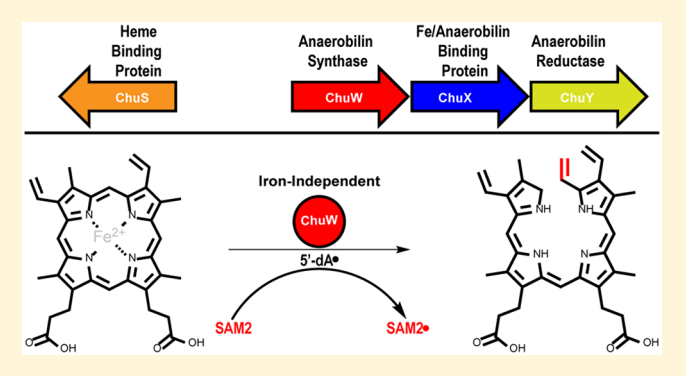
New Insight into the Mechanism of Anaerobic Heme Degradation

Liju G. Mathew, Nathaniel R. Beattie, Clayton Pritchett, and William N. Lanzilotta*

Department of Biochemistry and Molecular Biology & Center for Metalloenzyme Studies, University of Georgia, Athens, Georgia 30602, United States

Supporting Information

ABSTRACT: ChuW, ChuX, and ChuY are contiguous genes downstream from a single promoter that are expressed in the enteric pathogen Escherichia coli O157:H7 when iron is limiting. These genes, and the corresponding proteins, are part of a larger heme uptake and utilization operon that is common to several other enteric pathogens, such as Vibrio cholerae. The aerobic degradation of heme has been well characterized in humans and several pathogenic bacteria, including E. coli O157:H7, but only recently was it shown that ChuW catalyzes the anaerobic degradation of heme to release iron and produce a reactive tetrapyrrole termed "anaerobilin". ChuY has been shown to function as an anaerobilin reductase, in a role that parallels biliverdin reductase. In this work we have



employed biochemical and biophysical approaches to further interrogate the mechanism of the anaerobic degradation of heme. We demonstrate that the iron atom of the heme does not participate in the catalytic mechanism of ChuW and that S-adenosyl-Lmethionine binding induces conformational changes that favor catalysis. In addition, we show that ChuX and ChuY have synergistic and additive effects on the turnover rate of ChuW. Finally, we have found that ChuS is an effective source of heme or protoporphyrin IX for ChuW under anaerobic conditions. These data indicate that ChuS may have dual functionality in vivo. Specifically, ChuS serves as a heme oxygenase during aerobic metabolism of heme but functions as a cytoplasmic heme storage protein under anaerobic conditions, akin to what has been shown for PhuS (45% sequence identity) from Pseudomonas aeruginosa.

or decades biochemistry textbooks espoused the function of S-adenosyl-L-methionine (SAM) as an important methyl donor in strictly S_N2-catalyzed methyl transfer reactions. This paradigm changed significantly with the identification and characterization of the radical SAM (RS) superfamily and the utilization of SAM in the generation of a highly reactive radical intermediate. 1-3 Our understanding of the radical generation mechanism by RS enzymes has come a long way over the past two decades, and more recently it has been shown that reductive cleavage of SAM, by a catalytically conserved [4Fe-4S] cluster, involves an organometallic intermediate. 4-6 The latter discovery brings the field full circle considering early investigations that compared RS enzymes to what was known about the mechanism of B₁₂-dependent enzymes. Following these initial investigations, extensive work has demonstrated that RS enzymes exert an astonishing amount of control in "tuning" the initial radical as well as guiding multiple radical intermediates during catalysis (-) allowing these enzymes to do far more than simply catalyze the anaerobic equivalent of essential oxygen-dependent reactions.

Paradoxically, it has also been discovered that a subclass of RS enzymes utilizes SAM as a methyl donor in addition to using SAM for radical generation. 10 Currently four distinct classes of RS methyltransferases (RSMTs) have been

identified. 10-13 Each RSMT class utilizes a distinct cofactor/ cosubstrate repertoire to facilitate notably different methyl transfer reactions. In general, RSMTs are involved in the methylation of inert carbon or phosphorus centers, hence the requirement for a radical intermediate. The mechanism of class A RSMTs, in the methylation of RNA bases, has been understood for some time and involves two strictly conserved cysteine residues to facilitate the methylation of sp²-hybridized carbon centers. 14-18 The class B RSMTs require a cobalamin cofactor to facilitate the methylation reaction and include enzymes such as CysS, ¹⁹ Fom3, ^{20,21} GenK, ²² PoyC, ²³ Sven0516,²⁴ and ThnK.²⁵ Class B RSMTs are more diverse, catalyzing the methylation of phosphonate phosphorus atoms as well as sp²- and sp³-hybridized carbon centers. Class C, or "HemN-like", RSMTs complete the methylation of sp²hybridized carbon centers without using cysteine residues. ²⁶⁻³² The vast majority of class C RSMTs are involved in the biosynthesis of natural products, with one notable exception.³³ Finally, the class D RSMTs use methylenetetrahydrofolate as a methyl donor³⁴ and function in methanopterin biosynthesis.

Received: September 12, 2019 Revised: October 22, 2019 Published: October 25, 2019

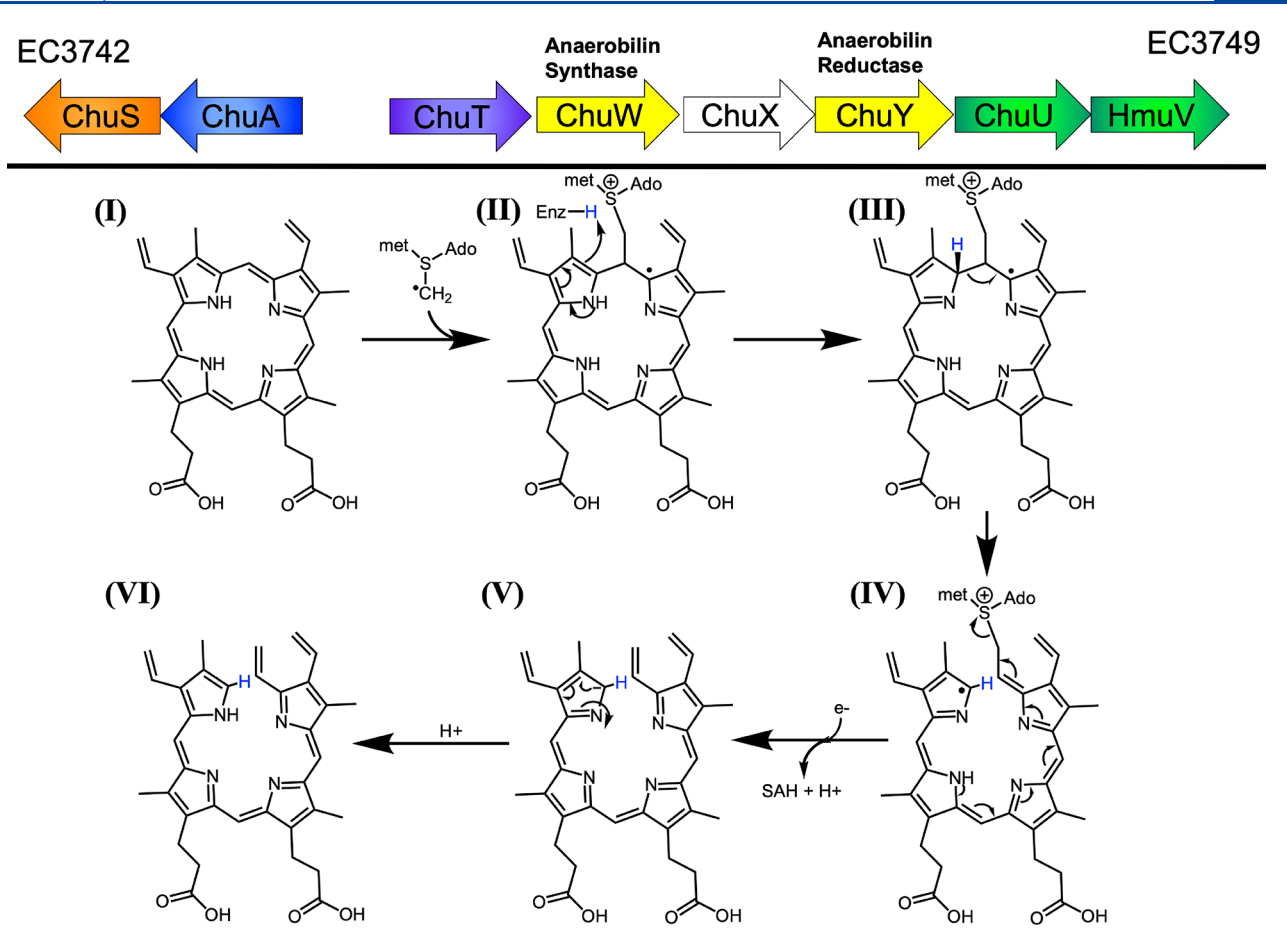


Figure 1. Heme utilization operon in *E. coli* O157:H7 (upper panel) and proposed metal-independent mechanism for ChuW (lower panel). In the proposed mechanism, the iron atom of the physiological substrate (heme) is not required for catalysis and *β*-scission of the porphyrin ring occurs prior to scission of the sulfur—carbon bond. Consistent with other RS enzymes, reductive cleavage of one SAM molecule results in generation of a 5′-deoxyadenosyl radical (5′-dA·). The 5′-dA· then abstracts a hydrogen atom from a second SAM molecule to generate a methylene radical that will add to the *meso* carbon atom of the porphyrin ring (I \rightarrow II). Protonation of the porphyrin ring (II \rightarrow III) will facilitate a *β*-scission reaction (III \rightarrow IV) and accounts for the incorporation of a single, nonexchangeable, proton in the anaerobilin product as has been previously observed. Further reduction, hydride formation (V), and protonation quench the radical and complete the reaction.

Of all the classes, the class C and D RSMTs are currently the least understood.

In this work, we address several unanswered questions regarding the mechanism of ChuW, a class C RSMT that was recently identified in the anaerobic degradation of heme by the enterohemorrhagic serotype Escherichia coli O157:H7.33 In fact, ChuW, ChuX, and ChuY are all expressed as part of a previously identified heme uptake and utilization operon (Figure 1).35 The expression of ChuW, ChuX, and ChuY is under the control of the fur promoter, and ChuW has been shown to catalyze the oxygen-independent opening of iron-protoporphyrin IX (heme).³³ The physiological role of this gene cluster is the liberation of iron during colonization and infection of the intestine.³⁵ However, unlike the canonical heme oxygenase reaction, ChuW utilizes an oxidative carbon radical to initiate and ultimately catalyze the opening of the porphyrin macrocycle. On the basis of observations with other RSMTs, we now propose that the metal ion does not participate in the mechanism of ring opening (Figure 1). Like the product of aerobic heme degradation (biliverdin), the product of anaerobic heme degradation, termed "anaerobilin", is a hydrophobic tetrapyrrole with potentially toxic properties. Hence, in a role analogous to biliverdin reductase, it has been shown that ChuY catalyzes the NADPH-dependent reduction

of anaerobilin.³⁶ The parallels to heme oxygenase and biliverdin reductase function are striking and suggest that accumulation of anaerobilin may be toxic to the pathogen. Consistent with this hypothesis, deletion of ChuY from the enterohemorrhagic E. coli CFT073 has been shown to result in a decrease in infectivity of the pathogen.³⁷ These data clearly indicate that ChuW and ChuY must function synergistically in vivo during anaerobic heme degradation by the pathogen and raise new questions about the function of ChuX, a protein expressed from the same operon from a gene (chuX) located between the chuW and chuY genes (Figure 1). Turnover of ChuW in D2O results in the incorporation of a single, nonexchangeable, deuterium atom. Therefore, our preferred mechanism involves transient formation of a hydride and, depending on which C-C bond is broken, formation of one of potentially two anaerobilin isomers. For simplicity only one product isomer of anaerobilin is shown in Figure 1.

Several additional questions regarding anaerobic heme degradation arise when other observations are considered. For example, cytoplasmic storage of external heme acquired by the pathogen is an open question. The *chuX* gene is located between *chuW* and *chuY*, and all three proteins are expressed at the same time. Previous work has reported that heme binds to ChuX with an affinity of 1.99 μ M.³⁸ However, the same

investigators have also shown that another cytosolic protein, ChuS, has a significant affinity ($\sim 1 \mu M$ under anaerobic conditions) for heme and can catalyze a peroxide-dependent heme degradation reaction in the presence of ascorbic acid and molecular oxygen.³⁹ More importantly, knockouts of the *chuS* homologue in Shigella dysenteriae, shuS, showed an impaired ability to utilize heme as an iron source at low heme (<15.0 μ M) levels with higher heme levels (>40.0 μ M) being lethal to the knockout strain. This is consistent with observations in other enteric pathogens that, without a "heme buffer", high cytosolic heme levels become toxic to the cell. 40 These data provide evidence that in the absence of molecular oxygen ShuS, and by homology ChuS, has an important role in heme storage in addition to the proposed role in heme degradation when molecular oxygen is present. 41 Specifically in the absence of molecular oxygen, a condition consistent with the colonization of the distal intestine, we propose that ChuS may function as a heme binding protein. This is consistent with the report that under anaerobic conditions ChuS binds heme ($K_d = 1.0 \mu M$) with greater affinity than ChuX.⁴¹ Under anaerobic conditions heme-loaded ChuS would be capable of storing heme as well as delivering heme to ChuW for degradation. Moreover, given the location and expression profile of ChuX, we hypothesize that this protein may function in a protein-protein complex with ChuW and ChuY during anaerobic heme degradation. Notably, a metal binding site has been identified in at least one other ChuX homologue (PDB ID 3FM2).

In this work we address several of these unanswered questions and hypotheses presented above, including whether the metal ion is required for opening the porphyrin ring. The data reported herein provides information about the biophysical properties of ChuW and sheds significant new light on the anaerobic heme degradation mechanism, including the identification of a catalytic residue. In addition, this investigation examines the roles of ChuS, ChuX, and their interactions with ChuW during anaerobic heme degradation. Evidence is presented that supports a new model wherein all four proteins work together in the anaerobic catabolism of heme.

■ MATERIALS AND METHODS

Expression, Purification, and Reconstitution. ChuW was expressed in E. coli BL21 DE3 using a commercially available pET expression plasmid exhibiting kanamycin resistance with an isopropyl β -D-1-thiogalactopyranoside (IPTG)-inducible promoter and a 6x his-tag. ChuW was coexpressed with the pDB1282 plasmid (ampicillin resistant) containing the isc operon during cell growth at low temperature. Briefly, a 20 mL starter culture was added to 2 L of M9 minimal media (4 L culture flasks) containing 0.02% casamino acids and grown at 37 °C, with shaking at 200 rpm. At an OD of 0.3, arabinose was added to 0.2% (wt/vol). At an OD₆₀₀ of 0.6, IPTG was added to a final concentration of 200 μ M, and cultures were incubated at 17 °C with shaking at 180 rpm for 17 h. Cells were harvested by centrifugation (10 000 × (g) and stored at -80 °C until further use. The cells were resuspended in degassed buffer (50 mM Tris buffer at pH 8.0 with 250 mM KCl, and 10% (v/v) glycerol containing DNase, Lysozyme, and PMSF) in an anaerobic glovebox, which was then sealed; the samples were then brought out of the glovebox to further degas with argon while being stirred. The solubilized cells were then lysed anaerobically by equilibrating a closedsystem French press with anaerobic buffer while maintaining a stream of argon in the drawing and collection flasks. The lysate was centrifuged at $60\,000 \times g$ for 1.5 h. The supernatant was collected, and ChuW was purified anaerobically by a gravity flow cobalt column equilibrated with buffer. The column was then washed with three column volumes of buffer containing 0 and 10 mM imidazole. ChuW was eluted in buffer containing 250 mM imidazole, and fractions were analyzed by SDS/ PAGE. The protein was then diluted to 1 mg/mL for reconstitution. Briefly, the protein was diluted in 50 mM Tris, pH 8.0, 250 mM KCl, 10% glycerol, and 5 mM DTT. After incubation for 5 min, 100 mM ferric chloride was added to 4 equiv of protein concentration while swirling. After a 30 min incubation, 15 μ L of 100 mM sodium sulfide was added every 10 min until reaching 1 equiv (eq) of the iron added. The mixture was capped and incubated in the glovebox for 12 h. The precipitate was removed by centrifugation, and the supernatant was run over a DEAE Sepharose anion exchange column by gravity flow in the glovebox. The column was washed with 20 mM Tris, pH 8.1, and 10% glycerol (buffer A), and the protein was eluted using a stepwise gradient of 1 M KCl in buffer A. Protein fractions were pooled, concentrated anaerobically, and stored in liquid nitrogen until further use.

Iron Analysis. Iron quantification of purified ChuW was performed using a colorimetric assay. Iron standards were prepared in acid-washed glassware at a concentration of 0.5 mM ferrous ammonium sulfate heptahydrate and diluted to various concentrations between 0.012 and 0.2 mM to a final volume of 250 μ L with identical buffers (20 mM Tris, pH 8.0, 300 mM KCl, and 10% glycerol). After acid precipitation and heat incubation at 80 $^{\circ}\text{C}$, 750 μL of $d\text{H}_{2}\text{O}$ was added, and then precipitates were pelleted by centrifugation; 750 μ L of each solution was transferred to a new microcentrifuge tube, where 50 μ L of 10% hydroxylamine and 250 μ L 0.1% bathophenanthroline were added with vortexing between additions. Samples were incubated at room temperature for 1 h and measured at 535 nm following the incubation period. ChuW samples were prepared in the same manner with triplicate measurements per concentration tested, whereas independent experiments were performed in triplicate as well. The same protocol was used to detect the total amount of iron available to the chelator in the ChuW assay before and after turnover. Any protein-bound iron is released during the acid hydrolysis and is subject to chelation by bathophenanthroline, whereas heme-, deuteroheme-, or mesoheme-bound iron is not.

UV-Vis Activity Assays. All UV-visible spectra were recorded on an HP 8453 diode array spectrophotometer running on OlisWorks using a Peltier temperature controller set to 25 °C and a stir speed of 1200 rpm. Typical enzyme assays were conducted anaerobically with degassed buffer containing 5% DMSO; 1 μ M ChuW; 5 μ M 3 E. coli Flavodoxin (flv); 2 μM E. coli NADP:Flavodoxin oxidoreductase (flx); 250 μ M NADPH; and 20 μ M of heme, protoporphyrin IX, deuteroheme, or deuteroporphyrin IX. Reactions were initiated by the addition of SAM to a final concentration of 250 μ M. Spectra were taken from 350 to 900 nm every 10 s for 30 min. Previously published extinction coefficients for DAB and anaerobilin were used to determine ChuW activity.³³ When determining the effect ChuX and ChuY had on ChuW activity, varying concentrations of the respective proteins were added to the assay mix prior to SAM addition. All data were fit and processed in either PRISM or Igor.

LC-MS Activity Assays. All LC-MS data was collected using an Orbitrap Q-TOF coupled to an Agilent 1500 HPLC system. For a standard 2 mL reaction mixture, titanium(III) citrate was added to a final concentration of 2 mM in 50 mM Tris buffer, pH 8.0 that also contained 150 mM KCl. ChuW and SAM were then added to a final concentration of 50 and 2 mM, respectively. The reaction mixture was then incubated for 5 min prior to the addition of porphyrin substrate. Heme, protoporphyrin IX, deuteroheme, or deuteroporphyrin IX was added to a final concentration of 250 µM. Reaction mixtures were covered and left in the dark overnight, with stirring. Following overnight incubation, the mixture was taken and added to DMSO, in a ratio of 2:1 DMSO to reaction buffer. The mixture was then spun down at $14800 \times g$ for 2 min to pellet precipitated protein. The supernatant was directly injected into an 88 µL injection loop prior to loading onto the column. An SAS-Hypersil C1 analytical column (150 \times 4.6 mm) from Thermo-Fisher was used for product separation. Separation was carried out using 100% methanol (solvent A) and 5 mM ammonium acetate pH 4.6 (solvent B) at a flow rate of 1.0 mL/min. Elution: start, 40% solvent A, 60% solvent B; 10 min, 73% solvent A, 27% solvent B; 20 min, 90% solvent A, 10% solvent B; 25 min, 95% solvent A, 5% solvent B. Total runtime was 30 min for each sample.

EPR Spectroscopy. Samples for electron paramagnetic (EPR) spectroscopy were prepared in an anerobic chamber where the oxygen concentration was maintained below 1 PPM at all times. EPR was used primarily as a "fingerprint" for the electronic environment of the [4Fe-4S] (formally 1+) cluster and to monitor SAM-dependent changes in the spectrum. Unless otherwise stated in the figure legend, all EPR spectra were recorded at 12 K with a microwave power of 0.1 mW and microwave frequency of 9.352 GHz, a modulation amplitude of 4.0 G, and modulation frequency of 100 kHz. Sodium dithionite was also included to a final concentration of 2 mM, in all the buffers used for EPR experiments. Samples were prepared in the anaerobic chamber, sealed, and then flash frozen in liquid nitrogen.

ChuX Alignment and Docking Studies. Alignment of the backbone α-carbon atoms for the ChuX protein from *E. coli* O157:H7 (PDB 2OVI, green), *A. variabilis* (PDB ID 3FM2, light blue), and *V. cholerae* HutX (PDB ID 5EXV, purple) was performed using PYMOL. ChuX from *E. coli* O157:H7 was used as the reference structure, and the maximum root-mean-square deviation (RMSD) that was obtained for any alignment described herein was 1.2 Å. This corresponded to the RMSD obtained when the model of HutX from *V. cholerae* was aligned with the ChuX model from *E. coli* O157:H7. In order to identify potential binding modes for anaerobilin binding to ChuX, we employed Autodock VINA⁴² using an energy-minimized model for anaerobilin generated with eLBOW.⁴³

Sedimentation Velocity Analysis. ChuX was dialyzed into 50 mM Tris buffer (pH 8) and 250 mM KCl for 24 h at 4 $^{\circ}$ C. The dialyzed protein was quantified on an Agilent 8453 spectrophotometer using an ε_{280} of 14 105 M $^{-1}$ cm $^{-1}$ as determined by ProtParam. The protein sample was diluted with the dialysis buffer to a final concentration of 0.72 mg/mL (4 μ M) and loaded into cells with 12 mm double-sector Epon centerpieces. The loaded cells were equilibrated in the rotor for 1 h at 20 $^{\circ}$ C, and sedimentation velocity data were collected at 50 000 rpm at 20 $^{\circ}$ C in an Optima XLA analytical ultracentrifuge. Data were recorded at 280 nm in radial step

sizes of 0.003 cm. SEDNTERP⁴⁵ was used to calculate the partial specific volume of ChuX (0.736638 mL/g) as well as the density (1.0114 g/mL) and viscosity coefficient (0.0101367) of the buffer. SEDFIT⁴⁶ was used to analyze the raw sedimentation data. Data were modeled as a continuous sedimentation coefficient distribution (c(s)) by fitting the baseline, meniscus, frictional coefficient, and systematic time-invariant and radial-invariant noise. The fit data for the experiment had a root-mean-square deviations of (rmsd) < 0.005 AU. The predicted sedimentation coefficient (s) values were calculated from the highest-resolution atomic coordinates of ChuX (PDB ID 6U9I) using HYDROPRO20.

ChuX and ChuY Expression and Purification. ChuX and ChuY were grown and purified under the same conditions. Each protein was expressed in E. coli BL21 DE3 cells using an IPTG-inducible expression plasmid with kanamycin resistance. LB media (1 L) was inoculated with a 20 mL starter culture, then grown at 37 $^{\circ}$ C with shaking at 200 rpm. At an OD₆₀₀ of 0.6, IPTG was added to a final concentration of 1 mM; cultures were then grown overnight at 17 °C. Cells were harvested by centrifugation before freezing and storage at -80 °C until further use. Frozen cell pellets were solubilized in buffer containing 50 mM Tris pH 8.0 250 mM KCl 10% glycerol with 0.05 mM PMSF, 0.05 mg/mL lysozyme, and 50 ug/mL DNase. Cells were lysed aerobically with a French pressure cell, and the lysate was centrifuged at 100 000g for 1.5 h. The supernatant was applied to TALON resin and washed with 2 column volumes of water and 8 column volumes of buffer. After the column was washed with 10 mM imidazole in buffer, protein was eluted with buffer containing 250 mM imidazole. Protein was analyzed by SDS-PAGE analysis and absorption at 280 nm prior to freezing at −80 °C for further

ChuS Expression, Purification, and Heme Reconstitution. ChuS expression and growth was the same as ChuX and ChuY procedures. Upon harvesting and freezing cells expressing ChuS, cells were solubilized anaerobically in 50 mM Tris pH 8.0 250 mM KCl 10% glycerol containing PMSF, DNase, and lysozyme. Cells continued to solubilize and degas under argon prior to anaerobic cell lysis as described above when purifying ChuW. Lysate was centrifuged at $100\,000 \times g$ for 1.5 h, then supernatant was loaded onto pre-equilibrated TALON resin. The column was washed with several column volumes of 10 mM imidazole prior to elution with 250 mM imidazole. Following elution, fractions containing ChuS were analyzed using SDS-PAGE then washed with buffer to remove imidazole prior to diluting to 5 mg/mL in buffer. Heme or PPIX stock solutions prepared in DMSO were added in 250 μL aliquots every 10 min with stirring to 5 equiv ChuS concentration. ChuS:Heme or ChuS:PPIX mixtures were concentrated to at least 1 mM prior to running over a preequilibrated (50 mM TRIS, 250 mM KCl, pH 8.0) Sephadex G-25 column to remove excess porphyrins. ChuS concentration was determined using absorption at 280 nm, and heme was determined to be 1:1 by using the previously published ChuS extinction coefficient $\varepsilon_{410} = 159 \text{ mM}^{-1} \cdot \text{cm}^{-1}$.

Site-Directed Mutagenesis of ChuW. Acidic amino acids that were predicted to be in the active site of ChuW and not in the conserved TIM barrel fold near the catalytic [4Fe-4S] cluster or cluster ligands were identified by structural modeling using PHYRE.² The predicted model and additional input from the conserved residues identified in a ClustalW sequence alignment of ChuW with HemN (PDB ID 1OLT) were used.

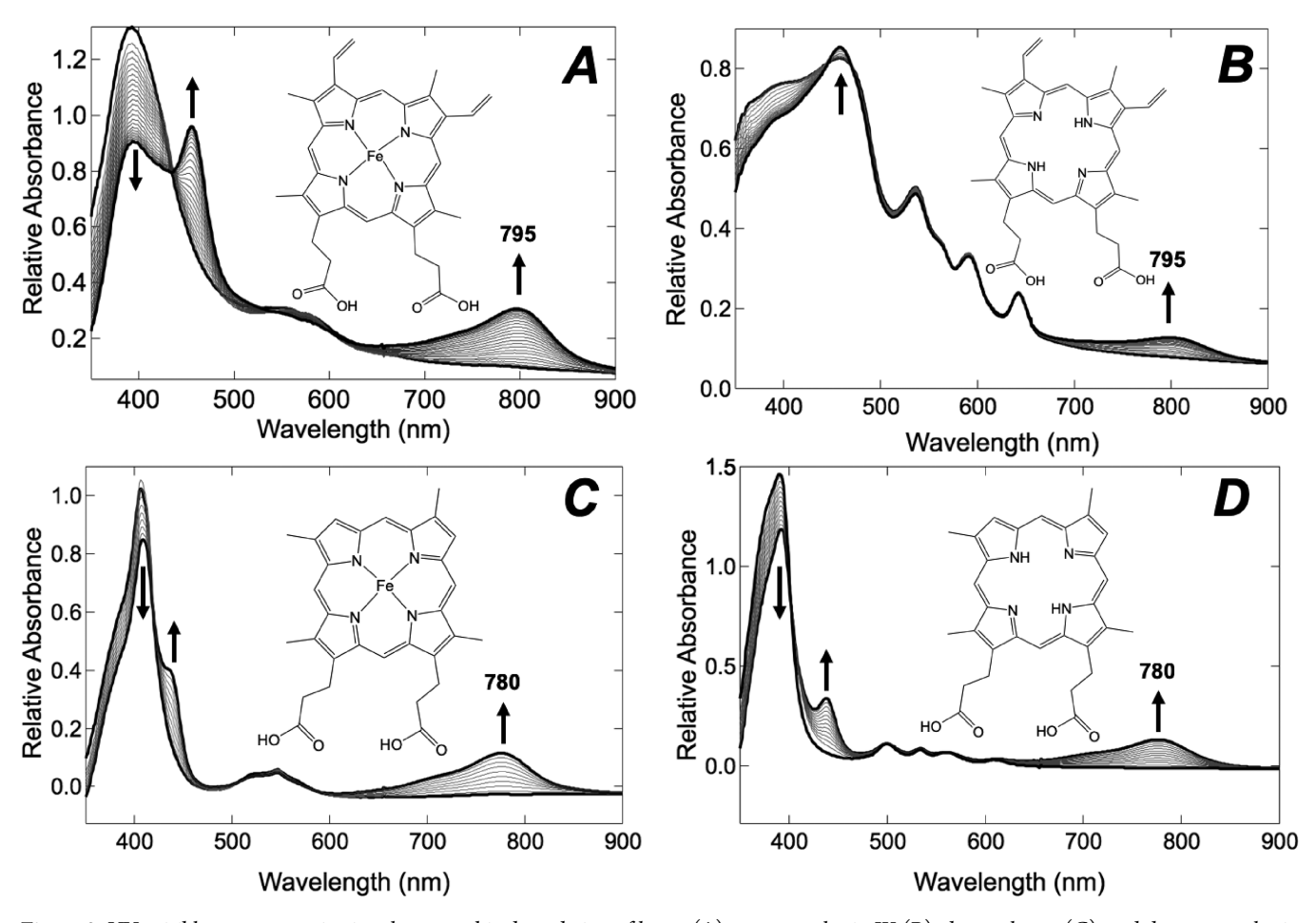


Figure 2. UV—visible spectra monitoring the anaerobic degradation of heme (A), protoporphyrin IX (B), deuteroheme (C), and deuteroporphyrin IX (D) catalyzed by ChuW. ChuW assays were performed as described in Materials and Methods. The structure of each substrate is shown as an inset in the respective panels, and the arrows indicate the direction of spectral changes during the assay.

Each mutation was engineered using Quickchange site-directed mutagenesis. In brief, complementary mutagenic oligonucleotide primers were designed to contain the desired mutation flanked by a 15-20 base pair extension on each end homologous to the parent plasmid. Each PCR reaction contained a total volume of 50 μ L with 4 μ M of each primer, 200 μ M of each dNTP, and 10 μ g of parent DNA, in ThermoPol reaction buffer (20 mM Tris-HCl (pH 8.8), 10 mM KCl, 10 mM (NH₄)₂SO₄, 2 mM MgSO₄, 0.1% Triton X-100). After preheating each condition at 95 °C for 5 min, 1.0 μL of Vent_R DNA Polymerase (New England Biolabs; #M0254S) was added to each tube, and the PCR reactions were allowed to proceed (annealing: 55-58 °C, 1 min; extension: 68-72 °C, 20 min; denaturing: 95 °C, 1 min; 18 complete cycles). Following the PCR reaction, 1.0 µL of DpnI (New England Biolabs; #R0176S) was added to each tube and allowed to react at 37 °C for 6 h. The suspensions were then transformed into competent BL21 DE3 E. coli, and identification of plasmids with the desired mutations was performed by subsequent isolation, PCR, and sequencing of plasmid DNA from candidate colonies.

RESULTS

Proposed Reaction Mechanism for ChuW. RS enzymes share a common mechanism for generation of the initial catalytic radical and have been shown to elicit an astonishing amount of control over radical intermediates during the course

of their catalytic mechanisms. 9,26,48 Therefore, although the physiological role of ChuW is to liberate iron from heme, we hypothesized that the iron atom does not participate in the catalytic mechanism of ChuW. This new proposal is outlined in Figure 1. Like other class C RSMTs we have presented evidence that ChuW utilizes two SAM molecules during a single turnover.³³ Moreover, the vast majority of RS enzymes utilize a catalytic [4Fe-4S] cluster to generate a 5'deoxyadenosyl radical (5'-dAdo·); therefore, the reaction mechanism shown in Figure 1 begins after the initial 5'dAdo· has abstracted a hydrogen atom from a second SAM molecule, leading to the formation of a transient methylene radical (Figure 1, I to II). Methylene radical addition to the conjugated ring system at the meso-carbon atom would proceed rapidly, leading to a covalent SAM-porphyrin adduct (Figure 1, intermediate II). Synthetic substrates that incorporate radical "traps" have proven extremely useful in previous work, 49 and an attempt to capture this adduct is underway using modified porphyrins. However, it should be noted that a similar adduct has been captured for the class C RSMT NosN.³¹ Breaking carbon–carbon bonds for sp²hybridized carbon atoms is thermodynamically difficult and, consistent with previous observations, ³³ protonation (Figure 1, intermediate III) to yield sp³-hybridization at both carbon atoms will lower the thermodynamic barrier, facilitating the β scission reaction (Figure 1, III to IV). At least one additional electron is required to complete the reaction scheme and

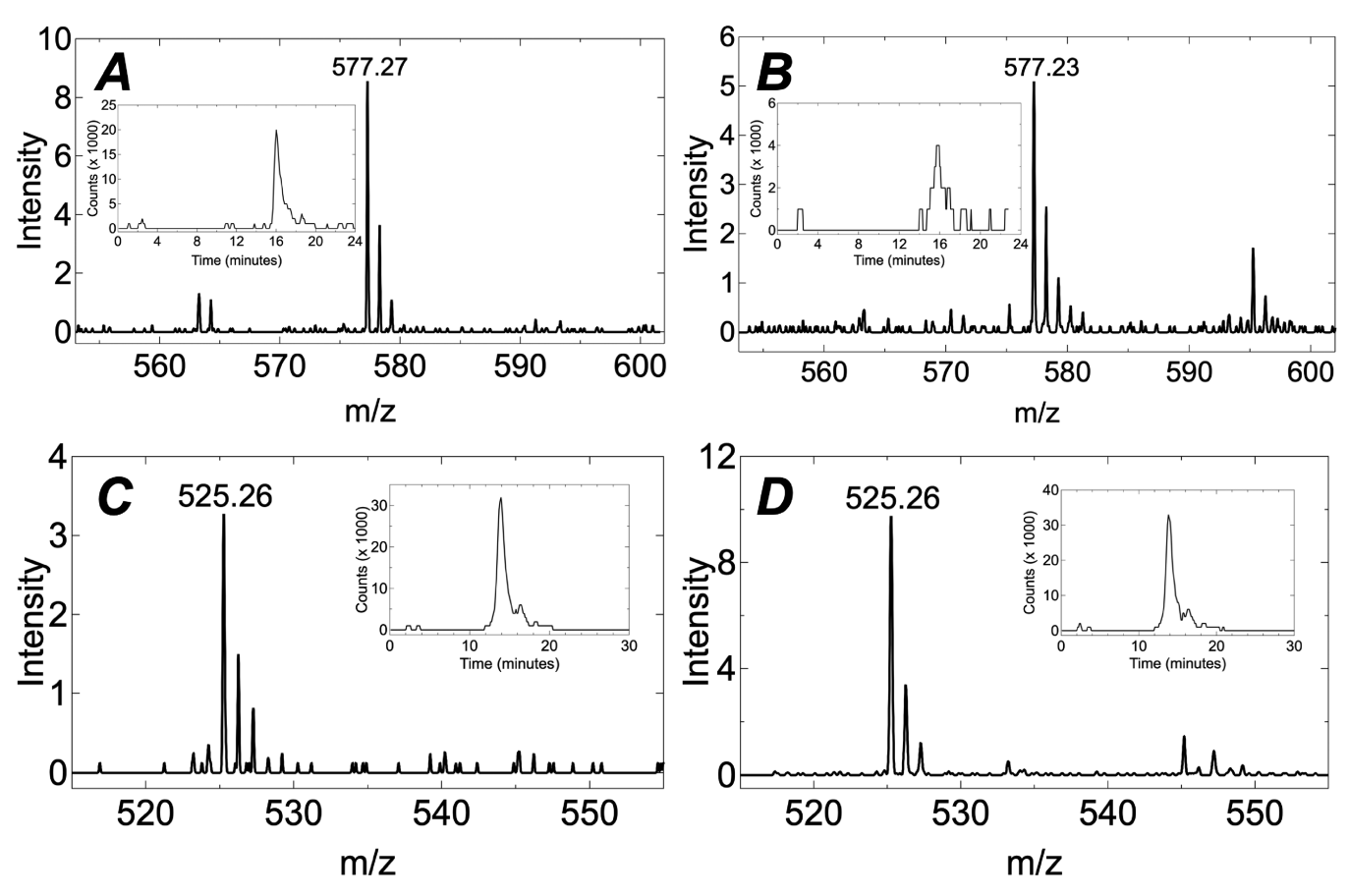


Figure 3. LC-MS analysis of ChuW turnover using heme (A), protoporphyrin IX (B), deuteroheme (C), or deuteroporphyrin IX (D) as the substrate. The reaction mixtures from each of the turnover assays shown in Figure 1 were analyzed by LC-MS as described in Materials and Methods. The extracted ion chromatogram for each product peak is shown in the panel inset.

produce the proposed tetrapyrrole structure that is consistent with the available mass spectroscopy data. ^{33,36} Initially, our hypothesis was that the iron atom of heme could facilitate additional electron transfer steps or even serve as the source of one electron because under physiological conditions the heme would most likely be in the ferrous state. However, given the catalytic precedent that has been set by several other RS enzymes it is also possible that the mechanism of ring opening is independent of any metal ion.

The Metal Ion Is Not Necessary for ChuW Catalysis. To address the potential role of the metal ion in the mechanism described above, the metal-free forms of both heme and deuteroheme, specifically protoporphyrin IX (PPIX) and deuteroporphyrin IX, were acquired and tested as substrates in the anaerobic degradation assay (Figure 2). All the porphyrin molecules (metalated as well as metal-free) investigated were acceptable substrates for ChuW. The metal-free porphyrins have notably different absorption spectra in the 450–600 nm range due to the lack of metal-porphyrin bonds, but the longer wavelength absorption feature of the linear tetrapyrrole product remains unchanged (795 nm for anaerobilin and 780 nm for deuteroanaerobilin). A significant challenge with these assays is the fact that the substrates are essentially insoluble in aqueous solutions, especially PPIX.

We address the solubility issue below by using the protein ChuS, also expressed when iron concentrations are low from a neighboring operon, as a "porphyrin carrier" for both heme and PPIX. Regardless, the absorption changes that we observe during the time course of the assay are consistent with

production of a similar product despite the type of substrate. In order to further address this, we also performed liquid column chromatography with mass spectroscopy (LC-MS) analysis on the turnover samples. As can be seen in Figure 3, when the turnover samples are analyzed by LC-MS, the extracted ion chromatograms and ion m/z data are the same whether the metalated or nonmetalated substrate is used.

Evidence for SAM-Dependent Conformational Changes in ChuW. HemN-like class C RSMTs require the binding of two SAM molecules,⁵⁰ in addition to the metabolic substrate that is being methylated and/or chemically modified. For ChuW, we have proposed that SAM binding induces conformational changes required for the proper orientation of heme and may involve changes in the coordination environment of the heme iron. Building on this hypothesis, a reasonable prediction would be that conformational changes associated with SAM binding increase the affinity for heme and/or may be required for efficient turnover. In addition, considering the damage uncontrolled radicals can cause, it would make sense to have a mechanism that prevents 5'-dAdogeneration in ChuW until both SAM and heme are bound. This proposal is not unique as it has long been recognized that enzymes can exist in multiple kinetic conformations;⁵¹ however, no evidence has been presented that addresses if this is occurring for ChuW. To investigate this further, we measured the rate of anaerobilin production after ChuW was preincubated with heme (Figure 4, top panel) or SAM (Figure 4, bottom panel). Progress curves tracking the production of anaerobilin can be monitored by following the appearance of

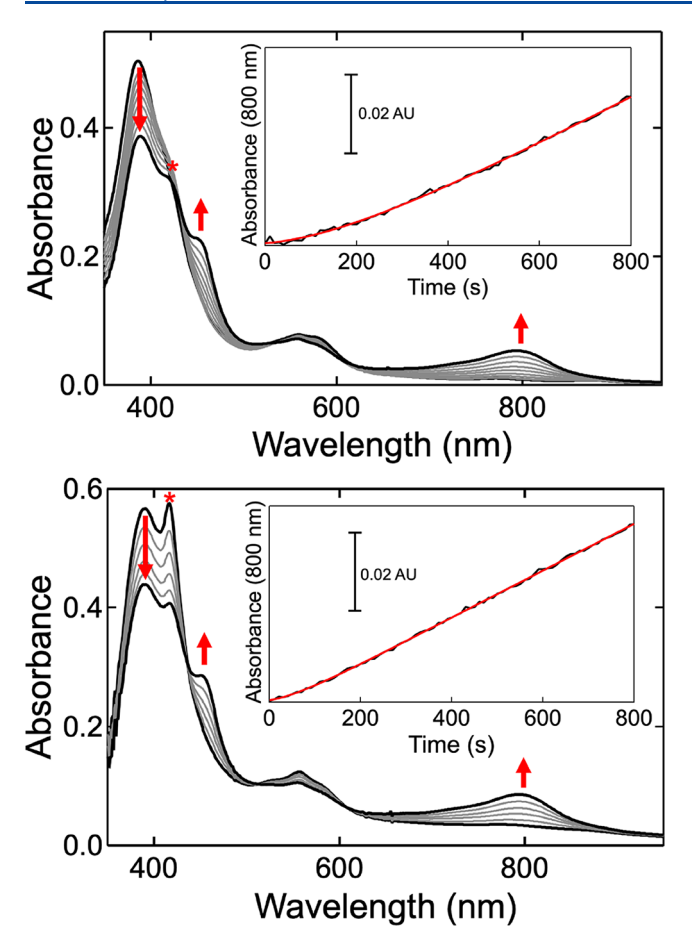


Figure 4. Progress curves monitoring heme turnover by ChuW without (top panel) and following (lower panel) preincubation with 1 mM SAM. Assays using 0.5 μ M ChuW were performed as previously descibed³³ except that, in the case of the data shown in the lower panel, 1 mM SAM was preincubated with ChuW for 5 min. In both cases the rate of product formation was followed by monitoring the appearance of the absorption feature at 795 nm (inset in both panels). Frieden's equation for describing a hysteretic enzyme was used to determine the lag time in both cases (red line fit) as described in the text. The asterisks highlight an absorption band, and potential intermediate, that is considerably more intense when ChuW is preincubated with SAM, prior to initiating the reaction.

the distinct anaerobilin absorption feature at 795 nm. The progress curves in Figure 4 reveal a significant hysteretic lag when ChuW is preincubated with heme, indicative of a slow transition from a less active to a more active conformation. The hysteretic lag, defined as the time taken for the enzyme to reach a steady-state velocity, can be determined by fitting the progress curves to the equation derived by Frieden: ⁵¹

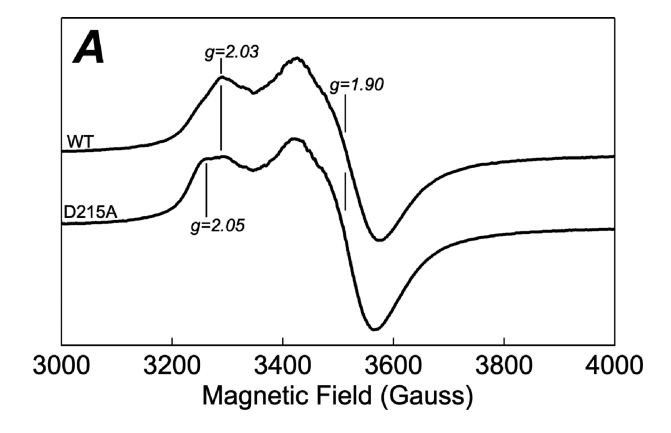
$$P(t) = v_{ss}t - \tau(v_{ss} - v_i)(1 - e^{-t/\tau})$$
(1)

P represents product concentration at time $t.\ \tau$ is equal to $1/k_{\rm obs}$, where $k_{\rm obs}$ is the apparent rate constant when transitioning from the initial velocity $(v_{\rm i})$ to the steady-state velocity $(v_{\rm ss})$. When preincubated with heme, ChuW exhibited a lag (calculated using lag = e\tau) of 1228 s. When preincubated with SAM, the lag time decreased markedly to 69 s. Additionally, SAM preincubation caused a red shift in the heme Soret band to 416 nm and increased intensity (Figure 4, asterisks), indicative of a heme-bound state existing immediately before turnover. This provides evidence for a SAM-

dependent transition from a less active to more active conformational state and is the first evidence of a distinct heme-bound intermediate that precedes catalysis.

Identification of a Catalytic Residue in ChuW. Consistent with the available data, the proposed mechanism for ChuW requires that a single nonexchangeable hydrogen atom, from water, is incorporated into anaerobilin.³³ Most likely, the proton transfer event is facilitated by an amino acid with solvent access, as shown in Figure 1. In order to address this, a homology model of ChuW was constructed using the online software PHYRE2.⁵² This model was structurally overlaid with the current HemN model (PDB ID 1OLT) containing two bound SAM molecules (Figure S1). Acidic amino acids that were predicted to be within 5-10 Å of the methyl group on the SAM molecule, not coordinating the [4Fe-4S] cluster, were targeted for mutagenesis. This included residues D18, D23, D215, D244, and E443. Alanine and the corresponding neutral mutations (asparagine or glutamine) were made at each position for a total of 10 ChuW variants. All variants, including the D215N ChuW, exhibited enzymatic activity except for the D215A variant. Therefore, characterization of the D215A ChuW variant was pursued. The D215A variant may not fold correctly resulting in the loss or incomplete incorporation of the catalytic [4Fe-4S] cluster. Hence, we investigated if the purified enzyme maintained structural stability and, in particular, whether the [4Fe-4S] cluster was intact. The EPR spectra of wild-type ChuW and the D215A variant are shown in Figure 5. Iron analysis of the purified enzymes indicated 3.7 and 3.5 iron atoms per peptide for the wild-type and D215A variant, respectively. Moreover, both enzymes exhibit an axial EPR spectrum that is consistent with the presence of the [4Fe-4S] cluster (Figure 5A) containing a single unpaired electron in an asymmetric environment. The addition of SAM is known to perturb that electronic environment because of coordination of a SAM molecule to the unique iron atom of the catalytic cluster.⁵³ As can be seen in Figure 5B, significant changes in the EPR spectrum are observed for both the wild-type ChuW and the D215A variant upon the addition of SAM. While the gvalues suggest that the D215A variant may contain multiple species, a cluster similar to the active enzyme clearly exists and is still capable of coordinating a SAM molecule. This indicates that D215A variant still contains a [4Fe-4S] cluster that is capable of binding the first SAM molecule. Therefore, the lack of activity must be due to subsequent steps in the reaction cycle, suggesting that D215 may have a catalytic role.

An Alternative Function for ChuX. The genes chuW, chuX, and chuY are found within the same operon and expressed behind the same promoter. Logic would therefore suggest that the corresponding proteins function together as part of a protein-protein complex. Similar to what has been proposed for ChuX, evidence has been presented that HutX, a homologue of ChuX in V. cholerae, may serve as a heme binding protein.⁵⁴ However, on the basis of computational modeling and structural analysis of several "X" proteins, we now propose an alternative function for ChuX. We have isolated and crystallized ChuX and, similar to what has been previously reported for both HutX and ChuX, 38,55 we observe a dimeric and tetrameric arrangement in our own ChuX crystals (Table S1, PDB ID 6U9J). However, the relevant question is what is the oligomeric structure of ChuX in solution? Sedimentation velocity analysis shows that a solution of 4 μ M ChuX exists primarily (81.3%) as a 2.9 S species that



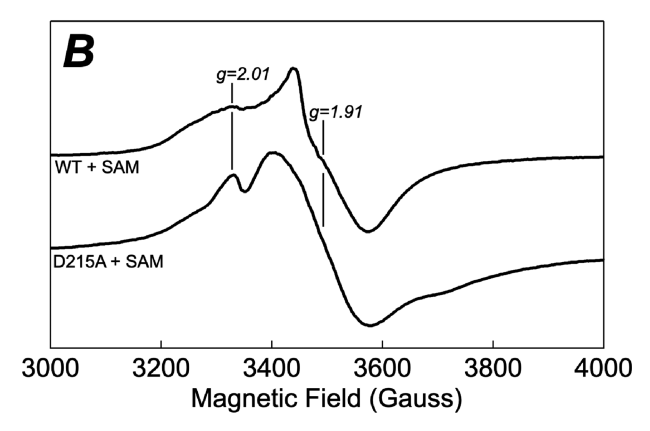
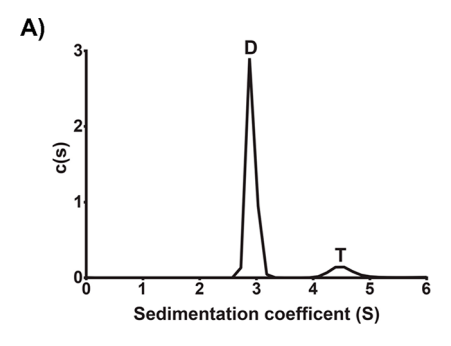


Figure 5. EPR spectra for the wild-type (WT) and D215A variant of ChuW in the absence (A) and presence of SAM (B). EPR spectra of 0.4 mM wild-type ChuW (WT) or the D215A variant (D215A) were recorded at 12 K in the absence (A) or presence of 1.0 mM SAM (B). Spectra were recorded at 12 K with a microwave power of 0.1 mW and microwave frequency of 9.352 GHz, a modulation amplitude of 4.0 G, and modulation frequency of 100 kHz. All spectra represent the sum of 10 scans.

is consistent with the predicted values for a dimer (2.8 S) (Figure 6). There is also a small amount (10.8%) of a 4.5 S species that agrees with the predicted value (4.4 S) of a tetramer (Figure 6A-C). This is consistent with the crystal packing where the dimer interface buries substantially more surface area (Figure 6B) when compared to the interface required to make the tetramer (Figure 6C). Specifically, a PISA analysis indicates a buried surface area of approximately 1000 $Å^2$ for the dimer interface (Figure 6A) while the other interface, required to complete the tetramer, buries approximately 500 Å² (Figure 6B,C). Moreover, the dimer interface is composed of numerous hydrophobic interactions surround by intrasubunit hydrogen bonds. These properties are hallmarks of a stable and permanent interface. In contrast, the interface that completes the tetramer consists predominantly of ionic interactions and hydrogen bonds.

Although both ChuX and HutX have been reported to bind heme with low micromolar affinities, no structural data has been obtained for either protein with heme bound. Figure 7 shows the structural alignment for *E. coli* O157:H7 ChuX (PDB ID 2OVI), *V. cholerae* HutX (PDB ID 5EXV), and *Anabaena variabilis* ChuX (PDB ID 3FM2). Interestingly, the *A. variabilis* ChuX structure also contained a Zn ion bound at two conserved amino acids (Figure 7, gray sphere). Given that the products (iron and anaerobilin) of the ChuW reaction are



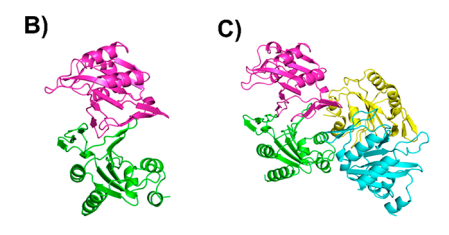


Figure 6. (A) Sedimentation velocity c(s) distribution of ChuX. Analysis was performed as described in Materials and Methods. ChuX was found to consist of a 2.9 S dimer (D) and 4.5 S tetramer (T). (B) ChuX dimer model colored by chain. C) ChuX tetramer model colored by chain. Both models were generated from the crystal structure (PDB ID 6U9J, Table S1).

both potentially toxic and the ChuY deletion strain showed a substantial decrease in infectivity,³⁷ we propose that ChuX may have an alternative function. Specifically, we propose that ChuX works synergistically with ChuW during the opening of the porphyrin ring and release of iron atom. In this role, ChuX would act as a chaperone to transiently sequester the iron atom and/or safely transfer the anaerobilin tetrapyrrole to ChuY, the anaerobilin reductase.³⁶ To address this new hypothesis, we performed a docking exercise using Autodock VINA. 42 The predicted docking mode for anaerobilin with the most favorable thermodynamic parameters is shown in Figure 7. Interestingly, the most favorable binding mode for anaerobilin binding to ChuX from E. coli O175:H7 is predicted to be proximal to the metal binding site observed in the crystal structure of ChuX from A. variabilis. Only the peptide atoms were present in the model during the docking simulation. However, it is notable that several of the observed (zinc binding) and predicted (anaerobilin) interactions involve conserved amino acids. Among these are E72 and H98 (E. coli numbering) involved in binding the zinc ion. The anaerobilin binding mode identified by Autodock also predicts a salt bridge with R112 and a ring stacking interaction with F136; both residues appear to be conserved in the other "X" homologues. These observations provide a framework to test our hypothesis that ChuX may serve as an iron/anaerobilin chaperone during the anaerobic heme degradation reaction catalyzed by ChuW.

ChuX and ChuY Stimulate ChuW Activity Synergistically. A logical starting point to address our new hypothesis regarding ChuX function is to test whether ChuX has any effect on the turnover rate we observe for ChuW. As a positive control we can add the anaerobilin reductase ChuY to the assay because product release (due to the low solubility of anaerobilin in aqueous solution) is the rate-limiting step. This has long been established to be the case for heme oxygenase; specifically, inclusion of biliverdin reductase in a heme oxygenase assay has been shown to significantly increase the

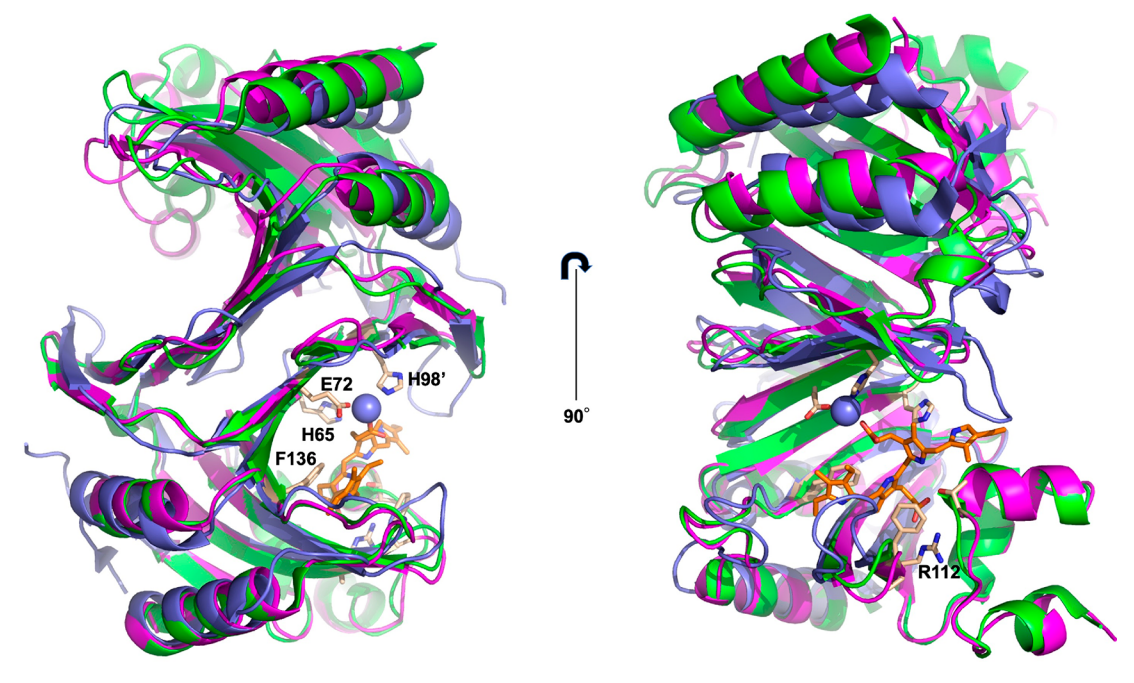


Figure 7. Cartoon representation showing a structural overlay for ChuX from *E. coli* O157:H7 (PDB pdb, green) aligned with the crystallographic models for ChuX from *A. variabilis* (PDB ID 3FM2, light blue), and *V. cholerae* HutX (PDB ID 5EXV, purple). Autodock VINA was used to predict the most favorable docking mode for the molecule anaerobilin (stick representation with orange carbon atoms) binding to ChuX from *E. coli* O157:H7 (orange stick representation). Interestingly, a zinc ion (light blue sphere) is observed in the crystallographic model for ChuX from *A. variabilis*. The zinc ion is bound by at least two conserved amino acids (E72 and H98 using *E. coli* ChuX numbering).

turnover rate. 56,57 Table 1 shows the changes in turnover rates when ChuY or ChuX are also included in the assay.

Table 1. Effect of ChuX and ChuY on the Rate of ChuW Heme Degradation Activity

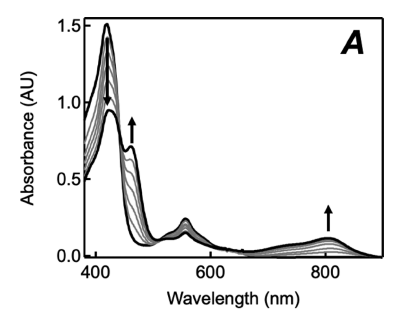
condition	specific activity ^a (nmol·min ⁻¹ ·mg ChuW ⁻¹)
ChuW alone	5.7 ± 0.3
ChuX:ChuW 4:1	16.9 ± 0.2
ChuY:ChuW 4:1	10.7 ± 0.2
ChuX:ChuY:ChuW 4:4:1	28.5 ± 0.5

^aSpecific activity determined by monitoring the degradation of heme. $\varepsilon_{402} = 51.63 \text{ mM}^{-1} \text{ cm}^{-1}$. Assay method is the same as that used in Figure 2, with the addition of varying concentrations of ChuX and ChuY.

The maximum effect seems to occur when the protein (ChuY or ChuX):ChuW ratios approached 4:1 (Figure S2). These results suggest that substrate release is also rate-limiting for ChuW and is in agreement with the function of ChuY as the next enzyme in the pathway (anaerobilin reductase). Unexpectedly, including both ChuX and ChuY resulted in an additive increase in the ChuW turnover rate (Table 1). The additive increase in the turnover rate indicates a more complex and synergistic interaction may be occurring between all three proteins.

ChuS Facilitates Heme or Protoporphyrin IX Transfer to ChuW during Anaerobic Porphyrin Degradation. In addition to ChuW, ChuX, and ChuY, ChuS is also expressed from an adjacent operon under iron-limiting conditions (Figure 1). Although the catabolites have not been isolated in vivo, purified ChuS has been shown to catalyze the peroxide-dependent degradation of heme to nonheme iron (bound to ShuS), tripyrrole (565 nm absorption), and

hematinic acid.⁵⁸ Of considerable significance is the observation that a homologous gene cluster and protein (ShuS) is found in the pathogen Shigella dysenteriae. Moreover, the S. dysenteriae ShuS knockout was shown to be defective in utilizing heme as an iron source under aerobic growth. 40 These findings confirm that ChuS provides a viable pathway for accessing heme iron in the presence of molecular oxygen, presumably as proposed by Ouellet et al.⁵⁸ However, under anaerobic conditions, ChuS binds heme but does not degrade it. In fact, under anaerobic conditions ChuS binds heme with a high affinity and heme-loaded ChuS can be isolated with substantial yields.^{39,41} We have found that heme-loaded ChuS is also quite stable and can be prepared at concentrations greater than 2.0 mM. Therefore, if heme can be transferred from ChuS to ChuW, it will be possible to use heme-loaded ChuS to increase the amount of substrate available to ChuW. The ability to use ChuS as a porphyrin source for ChuW has significant implications. In particular, this indicates ChuS can store excess heme under anaerobic conditions, protecting the cell. Moreover, increasing substrate availability to ChuW is essential to future spectroscopic investigations such as rapid freeze-quench electron paramagnetic resonance (RFQ-EPR) studies aimed at trapping and identifying the proposed radical intermediates. To this end, we have prepared heme-bound ChuS following the previously reported protocols^{39,41,58} and found that it can deliver heme to ChuW in our anaerobic assay (Figure 8A). The spectral changes we observe in Figure 3 are consistent with anaerobilin formation based on the increase in absorption at 445 and 795 nm (Figure 8A). As expected, the reaction still required the physiological electron delivery system (E. coli flavodoxin and NADPH-flavodoxin/oxidoreductase) and SAM. Moreover, none of the absorption changes resemble the previously reported tripyrrole product⁴² that was observed for the aerobic heme degradation reaction.



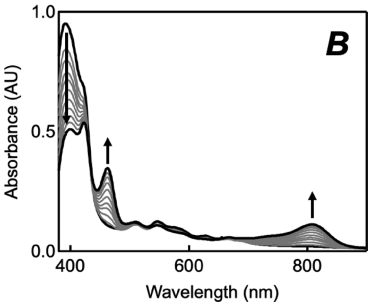


Figure 8. UV—visible spectra monitoring the degradation of heme (A) or protoporphyrin IX (B) catalyzed by ChuW when ChuS is utilized as the porphyrin carrier. The anaerobic degradation assay was performed as described in Materials and Methods, except that either heme- or protoporphyrin IX- loaded ChuS was utilized as the substrate (10 μ M). Heme-loaded ChuS was prepared as described by Suits et al. ³⁹ and utilized in place of free heme. Protoporphyrin IX-loaded ChuS was prepared by the same protocol. Arrows indicate the direction of spectral changes during the assay. The broad absorption band at 800 nm is indicative of the formation of anaerobilin.

Because ChuS could effectively deliver heme to ChuW, and protoporphyrin IX (PPIX) is also viable substrate, we tested whether PPIX-loaded ChuS could be used to provide the metal-free substrate, PPIX, to ChuW during turnover (Figure 8B).

This observation is significant for primarily two reasons. First, a viable attempt to capture and analyze radical intermediates will require that those intermediates are present as a substantial percentage of the total population of states in the sample. Increasing the amount of substrate available to ChuW will be an important step toward achieving this goal. In addition, PPIX does not contain a paramagnetic metal ion, thus preventing any additional spin-coupling with radical intermediates that would otherwise prevent detection and/or complicate data interpretation. As can be seen in Figure 8B, PPIX-loaded ChuS was also a viable way to deliver the porphyrin substrate to ChuW and resulted in turnover based on the changes seen in the UV-visible spectrum. Taken together, these data indicate that ChuS has a role in heme storage and delivery to ChuW under anaerobic conditions. The application of ChuS, as a means for increasing the availability of substrate (either heme or PPIX) to ChuW will also facilitate future spectroscopic studies aimed at dissecting the radical cleavage mechanism.

DISCUSSION

In this work, we provide new mechanistic insight into the anaerobic heme degradation pathway in *E. coli* O157:H7 using activity assays, LC-MS analysis, biophysical approaches, and docking studies. The data presented herein demonstrate unequivocally that the heme-iron is not essential to the

degradation mechanism catalyzed by ChuW. Evidence is also presented that reveals ChuW undergoes SAM-dependent conformational changes that influence the heme binding mode and facilitate catalysis. In addition, the assays reported here demonstrate a synergistic effect on ChuW activity when other proteins from the heme utilization operon are present. Specifically, evidence presented in this work indicates that ChuS and ChuX may have multiple functions depending on the metabolic state. A new model is proposed for the anaerobic heme degradation mechanism catalyzed by ChuW and discussed in the broader context of the class C radical SAM methyltransferase superfamily. This is important as class C RSMTs have been implicated in the biosynthesis of a number of natural products with important bioreactivity, but their catalytic mechanisms remain poorly understood. ⁵⁹

Mechanism of Ring Opening. Prior to turnover, we suspect that the proper orientation of both SAM molecules has important structural/functional consequences for all HemN-like class C RSMTs. As we demonstrate here, preincubation of ChuW with SAM results in a significantly shorter lag time as well as an increase in the Soret band at 417 nm that is transiently observed (Figure 4, red asterisks). The logical conclusion is that the SAM-dependent conformational changes take some time but result in a heme-bound state that is more catalytically competent. In this sense, the Soret at 417 nm will allow us to probe the heme-bound intermediate further using spectroscopic techniques such as resonance Raman in the future.

In general, radical SAM enzymes have been shown to control substrate-centered radicals in order to catalyze β scission reactions that cleave carbon-carbon and carbonnitrogen bonds. In some cases, multiple β -scission steps occur during the course of a single turnover, as has been reported for the enzyme ThiC.60 In the case of ChuW, primary sequence alignments as well as the mechanistic properties indicate that this enzyme belongs to the "HemN-like" or class C RSMT subfamily. In particular, two molecules of SAM are required per turnover.³³ The first SAM molecule generates the initial 5'dAdo-, ultimately resulting in formation of methionine and 5'deoxyadenosine, while the second molecule of SAM facilitates a methyl transfer step, resulting in production of S-adenosyl-Lhomocysteine (SAH). Previous work with ChuW has provided evidence that the 5'-dAdo· abstracts a hydrogen atom from the second SAM molecule to form a methylene radical. Addition of this radical species to the conjugated ring system at the bridging meso carbon atom would result in a transient SAMporphyrin adduct (Figure 1, intermediate II). Evidence for similar SAM-substrate adducts during turnover has been observed for other HemN-like class C RSMTs such as Jaw5,50 NosN,31 and HemN,61 suggesting that this is a common mechanistic feature of all class C RSMTs.

The thermodynamics for breaking a C–C bond by β -scission, radical-catalyzed or otherwise, are considerably more favorable if both carbon atoms are sp³ hybridized, and therefore, we favor a mechanism involving protonation/hydride formation. This is also consistent with the incorporation of a single nonexchangeable deuteron that we observe when ChuW turnover is perform in D₂O. The protonation event may be facilitated by an amino acid in the active site, and therefore, we investigated amino acids that could function in this role. It is tempting to conclude that D215 may be involved in the protonation event because the D215A variant is inactive. However, because the D215N variant is still active there are

other possible explanations. In fact, an asparagine residue would be capable of hydrogen bonding and would also occupy the same physical space as an aspartic acid group. Therefore, while D215 could be involved in an important hydrogen bonding network, a more attractive explanation is that D215 is involved in the orientation of the second SAM molecule within the active site of ChuW. In this case, the D215N variant is still capable of fulfilling a hydrogen bond required to orient the second SAM molecule, allowing catalysis to proceed. While SAH is already a good leaving group, it is important to note that a general base has been implicated in other class C RSMTs in order to facilitate the elimination reaction. 31,32 The porphyrin ring is essentially electron-rich and proton-deficient. In fact, if the ratio of π and lone pair electrons, relative to the total number of protons, is considered, one gets a sense of just how aromatic or electron-rich a compound is. Using this analysis, the electron:proton ratio of a single pyrrole ring is 0.1935, essentially making the pyrrole group more aromatic than benzene (electron:proton ratio of 0.167). Although we cannot eliminate the possibility that a general base facilitates the elimination of SAH, as has been proposed for NosN and TbtI, 31,32 if a similar mechanism is at work in ChuW, then one significant difference would be that SAH is lost prior to C-C bond cleavage.

Regardless of whether the β -scission reaction catalyzed by ChuW involves formation of a hydride (Figure 1) or utilizes a general base, the reaction will require an additional electron to quench the radical species and complete the reaction. While this work eliminates the possibility that the heme iron provides an electron or plays a role in catalysis, it is possible that the [4Fe-4S] cluster could facilitate additional NADPH-dependent electron transfer via flavodoxin or ferredoxin. We know that heme oxygenases receive subsequent electrons necessary for heme degradation from NADPH-cytochrome P450 reductase (CPR), the physiological redox partner. For radical SAM enzymes this is a particularly important point because the electron donor has been shown to influence the catalytic reaction.⁶² Artificial electron donors such as titanium(III)citrate are preferred because other chemical reductants have led to catalytic artifacts such as the "abortive cleavage" of SAM when sodium dithionite is used as the reductant.6

Multiple Functions for ChuX and ChuS. ChuX (HutX in V. cholerae) is a small peptide that has been annotated as a heme binding protein.^{38,54} Interestingly, ChuS is essentially a tandem repeat of two "ChuX-like" domains. However, structural alignment of the ChuX dimer on the published ChuS model (PDB ID 4CDP) with heme bound yields an RMSD of 4.8 Å, with no equivalent heme-ligating residues seen in ChuX. Alignment of only the heme binding domains improves the RMSD to 2.2 Å. Despite the similar affinities for heme that have been reported for ChuX and ChuS, only the heme-bound form of ChuS has been characterized structurally. While ChuS may function as a heme oxygenase in the presence of molecular oxygen, this work clearly supports a role in heme storage and transport to ChuW under anaerobic conditions. Moreover, the protein PhuS from the enteric pathogen Pseudomonas aeruginosa shares 45% sequence identity with ChuS and has clearly been shown to play a role in cytoplasmic heme storage.⁶⁴ Having proteins that can serve multiple functions is not uncommon and will provide the pathogen with a selective advantage. In particular, given the toxicity of heme, a role in sequestering heme under anaerobic (reducing) conditions would be beneficial. We therefore propose that

ChuS, like PhuS, also has a role in heme storage under anaerobic growth conditions.

HutX from V. cholerae, like ChuX, has been reported to bind the hydrophobic heme molecule. In both organisms, ChuX and HutX are transcribed from the gene immediately following ChuW and HutW, respectively. It stands to reason that the breakdown product of anaerobic heme degradation in both organisms is a hydrophobic tetrapyrrole that is chemically reactive and therefore toxic. Deletion of ChuY, the anaerobilin reductase, resulted in a phenotype that is consistent with this hypothesis.³⁷ In fact, the only deletions that have been shown to lead to a fitness phenotype, during growth on heme as the sole iron source, in pathogenic E. coli or V. cholerae, are deletion of ChuY or HutZ, respectively. 37,65 Moreover, the observations reported here demonstrate that both ChuX and ChuY stimulate ChuW activity individually as well as in an additive manner. This observation is consistent with ChuX playing a role in binding anaerobilin prior to ChuY (HutZ in V. cholerae) performing the NADPH-dependent reduction of anaerobilin. The ultimate goal of heme degradation in pathogenic bacteria is to liberate iron, yet iron's fate following turnover is a significant question that requires further investigation. Whether ChuX also facilitates the safe removal, storage, and transport of iron and anaerobilin is under further investigation, but this proposal is consistent with the organization of the genes within the heme utilization operon and the stimulation of activity that we have observed. Moreover, structural alignment of ChuX from E. coli O157:H7 with homologues in V. cholerae and A. variabilis identifies a potential metal binding site. Two conserved amino acids, a glutamate and histidine, coordinate a Zn ion in the A. variabilis structure (PDB ID 3FM2). It stands to reason that anaerobilin and iron are cytotoxic molecules. In fact, the proposed anaerobilin molecule is markedly more hydrophobic than biliverdin (product of canonical heme oxygenase), and product release has long been known to be the rate-limiting step in the heme oxygenase reaction. 56 The increased hydrophobicity may further slow product release from the ChuW active site, necessitating the use of a transporter/ chaperone like ChuX or HutX in V. cholerae. Whether HutW in V. cholerae performs a heme-degradation reaction that is similar to ChuW is currently under investigation.

Turnover of Nonmetalated Porphyrins. The observation that ChuW will utilize nonmetalated substrates, such as protoporphyrin IX and deuteroporphyrin IX, provides a means to further probe the ChuW mechanism by spectroscopic means without the complication of an additional paramagnetic center, further advancing our understanding of class C RSMTs. Although heme-iron liberation is the physiological goal of this system, we have shown that the heme-iron itself is not essential to the ring-opening reaction catalyzed by ChuW. The product features associated with anaerobilin formation at 456 and 795 nm form over time with clear isosbestic points when heme or protoporphyrin IX is incubated with reduced ChuW (Figure 2; compare panels A and B). The same holds true when incubating deuteroheme or deuteroporphyrin IX with reduced ChuW, forming a product consistent with deuteroanaerobilin at 439 and 780 nm (Figure 2; compare panels C and D). LC-MS analysis corroborates the UV-vis assay data, demonstrating the same products are formed when degrading metalated porphyrins or their nonmetalated counterparts (Figure 3). ChuW can degrade heme and protoporphyrin IX to anaerobilin, consistent with a product at 577 m/z that eluted

at 16 min (Figure 3A,B). The product intensity is noticeably weaker when using protoporphyrin IX as a substrate and can be attributed to its increased insolubility in aqueous solution. ChuW was also able to degrade deuteroheme and deuteroporphyrin IX to DAB, consistent with a product at $525 \ m/z$ that eluted at 14 min (Figure 3C,D). The product masses observed were consistent with previously reported work, and together the UV—vis and LC-MS data demonstrate the metal is not involved in the degradation mechanism. All of these observations support the use of the nonmetalated substrates for future spectroscopic investigations aimed at trapping and characterizing radical intermediates.

CONCLUSIONS

Radical SAM (RS) enzymes continue to be identified that expand the catalytic diversity of the superfamily and the mechanism(s) by which the peptide environment controls radical catalysis. ChuW belongs to the "HemN-like", or class C RSMT, subfamily of RS enzymes, and although this subfamily is the least understood, our work supports some core mechanistic principles. Specifically, that HemN-like RS enzymes require two SAM molecules to function. The first SAM molecule generates the catalytic radical, presumably via the "omega species", that abstracts a hydrogen atom from the second SAM molecule to form a methylene radical. The methylene radical attacks a double bond on a nearby substrate that may undergo substantial radical rearrangements in subsequent steps.

For ChuW, the implication that additional proteins, such as ChuX or ChuS, have multiple roles or function synergistically as part of a protein-protein complex in vivo is intriguing. In particular, if enzymes in this subfamily do function as part of larger complexes then this may explain some experimental inconsistencies and the utility of the protein fold as a heme chaperone. For example, HemW is one such HemN-like protein that has been shown to be a heme chaperone but that is also still capable of SAM cleavage.⁶⁶ In this case, the precise role of SAM binding and cleavage is not clear. One possible explanation is that other proteins interact with HemW for in vivo function with heme transfer requiring SAM cleavage. Regardless, for persistent enteric pathogens that can utilize heme as an iron source, heme and the breakdown products of heme will have certain toxic effects. The data presented in this work support a new model whereby ChuS, ChuW, ChuX, and ChuY function together to ensure the safe and efficient catabolism of heme under anaerobic conditions when iron is limiting.

ASSOCIATED CONTENT

S Supporting Information

The Supporting Information is available free of charge on the ACS Publications website at DOI: 10.1021/acs.biochem.9b00841.

Data collection and refinement statistics for the ChuX model, the homology model we have generated for ChuW using PHYRE2, as well as the biochemical assay data (PDF)

Accession Codes

The atomic coordinates and structure factors for the ChuX model discussed in this work have been deposited in the Protein Data Bank as entry 6U9J. Information on the enzymes being studied in this work can be found under the UniProt IDs

Q8X5N8, A0A384LP51, Q9KL40, and Q8X5N4 for ChuS, ChuW, ChuX, and ChuY, respectively.

AUTHOR INFORMATION

Corresponding Author

*Phone: (706) 542-1324. Fax: (706) 542-1738. E-mail: wlanzilo@uga.edu.

ORCID ®

William N. Lanzilotta: 0000-0002-4852-321X

Funding

Funding from the National Institute of General Medical Sciences (Grant R01GM124203) to W.N.L. is gratefully acknowledged. The authors also acknowledge that funding for the EMXplus EPR and cryogen-free Stinger cooling system was provided by a grant from the NSF Major Research Instrumentation (MRI) program in the Division of Chemistry (CHE-1827968).

Notes

The authors declare no competing financial interest.

ACKNOWLEDGMENTS

The authors acknowledge Dr. Zachary A. Wood for helpful discussions and assistance with interpretation of the AUC data. The authors thank the staff at the Southeast Regional Collaborative Access Team (SER-CAT) at the Advanced Photon Source, which is supported in part by the National Institutes of Health (S10 RR25528 and S10 RR028976). The authors also acknowledge the National Institute of General Medical Sciences for an equipment grant supporting our inhouse X-ray facility (S10 OD021762).

REFERENCES

- (1) Broderick, J. B., Duffus, B. R., Duschene, K. S., and Shepard, E. M. (2014) Radical S-adenosylmethionine enzymes. *Chem. Rev.* 114, 4229–4317.
- (2) Frey, P. A., and Booker, S. J. (2001) Radical mechanisms of Sadenosylmethionine-dependent enzymes. *Adv. Protein Chem.* 58, 1–45
- (3) Buckel, W., and Golding, B. T. (2006) Radical enzymes in anaerobes. *Annu. Rev. Microbiol.* 60, 27–49.
- (4) Horitani, M., Shisler, K., Broderick, W. E., Hutcheson, R. U., Duschene, K. S., Marts, A. R., Hoffman, B. M., and Broderick, J. B. (2016) Radical SAM catalysis via an organometallic intermediate with an Fe-[5'-C]-deoxyadenosyl bond. *Science* 352, 822–825.
- (5) Byer, A. S., Yang, H., McDaniel, E. C., Kathiresan, V., Impano, S., Pagnier, A., Watts, H., Denler, C., Vagstad, A. L., Piel, J., Duschene, K. S., Shepard, E. M., Shields, T. P., Scott, L. G., Lilla, E. A., Yokoyama, K., Broderick, W. E., Hoffman, B. M., and Broderick, J. B. (2018) Paradigm Shift for Radical S-Adenosyl-l-methionine Reactions: The Organometallic Intermediate Omega Is Central to Catalysis. *J. Am. Chem. Soc. 140*, 8634–8638.
- (6) Broderick, W. E., Hoffman, B. M., and Broderick, J. B. (2018) Mechanism of Radical Initiation in the Radical S-Adenosyllmethionine Superfamily. *Acc. Chem. Res.* 51, 2611–2619.
- (7) Mehta, A. P., Abdelwahed, S. H., Mahanta, N., Fedoseyenko, D., Philmus, B., Cooper, L. E., Liu, Y., Jhulki, I., Ealick, S. E., and Begley, T. P. (2015) Radical S-adenosylmethionine (SAM) enzymes in cofactor biosynthesis: a treasure trove of complex organic radical rearrangement reactions. *J. Biol. Chem.* 290, 3980–3986.
- (8) Gagnon, D. M., Stich, T. A., Mehta, A. P., Abdelwahed, S. H., Begley, T. P., and Britt, R. D. (2018) An Aminoimidazole Radical Intermediate in the Anaerobic Biosynthesis of the 5,6-Dimethylbenzimidazole Ligand to Vitamin B12. *J. Am. Chem. Soc.* 140, 12798–12807.

(9) Wang, Y., Schnell, B., Muller, R., and Begley, T. P. (2018) Iterative Methylations Resulting in the Biosynthesis of the t-Butyl Group Catalyzed by a B12-Dependent Radical SAM Enzyme in Cystobactamid Biosynthesis. *Methods Enzymol.* 606, 199–216.

- (10) Bauerle, M. R., Schwalm, E. L., and Booker, S. J. (2015) Mechanistic diversity of radical S-adenosylmethionine (SAM)-dependent methylation. *J. Biol. Chem.* 290, 3995–4002.
- (11) Ding, Y., Yu, Y., Pan, H., Guo, H., Li, Y., and Liu, W. (2010) Moving posttranslational modifications forward to biosynthesize the glycosylated thiopeptide nocathiacin I in Nocardia sp. ATCC202099. *Mol. BioSyst.* 6, 1180–1185.
- (12) Zhang, Q., van der Donk, W. A., and Liu, W. (2012) Radical-mediated enzymatic methylation: a tale of two SAMS. *Acc. Chem. Res.* 45, 555–564.
- (13) Fujimori, D. G. (2013) Radical SAM-mediated methylation reactions. *Curr. Opin. Chem. Biol.* 17, 597–604.
- (14) Yan, F., LaMarre, J. M., Röhrich, R., Wiesner, J., Jomaa, H., Mankin, A. S., and Fujimori, D. G. (2010) RlmN and Cfr are Radical SAM Enzymes Involved in Methylation of Ribosomal RNA. *J. Am. Chem. Soc.* 132, 3953–3964.
- (15) Boal, A. K., Grove, T. L., McLaughlin, M. I., Yennawar, N. H., Booker, S. J., and Rosenzweig, A. C. (2011) Structural basis for methyl transfer by a radical SAM enzyme. *Science* 332, 1089–1092.
- (16) Grove, T. L., Benner, J. S., Radle, M. I., Ahlum, J. H., Landgraf, B. J., Krebs, C., and Booker, S. J. (2011) A radically different mechanism for S-adenosylmethionine-dependent methyltransferases. *Science* 332, 604–607.
- (17) Grove, T. L., Radle, M. I., Krebs, C., and Booker, S. J. (2011) Cfr and RlmN contain a single [4Fe-4S] cluster, which directs two distinct reactivities for S-adenosylmethionine: methyl transfer by SN2 displacement and radical generation. *J. Am. Chem. Soc.* 133, 19586–19589.
- (18) Schwalm, E. L., Grove, T. L., Booker, S. J., and Boal, A. K. (2016) Crystallographic capture of a radical S-adenosylmethionine enzyme in the act of modifying tRNA. *Science* 352, 309–312.
- (19) Wang, Y., Schnell, B., Baumann, S., Muller, R., and Begley, T. P. (2017) Biosynthesis of Branched Alkoxy Groups: Iterative Methyl Group Alkylation by a Cobalamin-Dependent Radical SAM Enzyme. *J. Am. Chem. Soc.* 139, 1742–1745.
- (20) Sato, S., Kudo, F., Kim, S. Y., Kuzuyama, T., and Eguchi, T. (2017) Methylcobalamin-Dependent Radical SAM C-Methyltransferase Fom3 Recognizes Cytidylyl-2-hydroxyethylphosphonate and Catalyzes the Nonstereoselective C-Methylation in Fosfomycin Biosynthesis. *Biochemistry* 56, 3519–3522.
- (21) Allen, K. D., and Wang, S. C. (2014) Initial characterization of Fom3 from Streptomyces wedmorensis: The methyltransferase in fosfomycin biosynthesis. *Arch. Biochem. Biophys.* 543, 67–73.
- (22) Kim, H. J., Liu, Y. N., McCarty, R. M., and Liu, H. W. (2017) Reaction Catalyzed by GenK, a Cobalamin-Dependent Radical S-Adenosyl-I-methionine Methyltransferase in the Biosynthetic Pathway of Gentamicin, Proceeds with Retention of Configuration. *J. Am. Chem. Soc.* 139, 16084–16087.
- (23) Parent, A., Guillot, A., Benjdia, A., Chartier, G., Leprince, J., and Berteau, O. (2016) The B12-Radical SAM Enzyme PoyC Catalyzes Valine Cbeta-Methylation during Polytheonamide Biosynthesis. *J. Am. Chem. Soc.* 138, 15515–15518.
- (24) Inahashi, Y., Zhou, S., Bibb, M. J., Song, L., Al-Bassam, M. M., Bibb, M. J., and Challis, G. L. (2017) Watasemycin biosynthesis in Streptomyces venezuelae: thiazoline C-methylation by a type B radical-SAM methylase homologue. *Chem. Sci.* 8, 2823–2831.
- (25) Marous, D. R., Lloyd, E. P., Buller, A. R., Moshos, K. A., Grove, T. L., Blaszczyk, A. J., Booker, S. J., and Townsend, C. A. (2015) Consecutive radical S-adenosylmethionine methylations form the ethyl side chain in thienamycin biosynthesis. *Proc. Natl. Acad. Sci. U. S. A. 112*, 10354–10358.
- (26) LaMattina, J. W., Wang, B., Badding, E. D., Gadsby, L. K., Grove, T. L., and Booker, J. (2017) NosN, a Radical S-Adenosylmethionine Methylase, Catalyzes Both C1 Transfer and

Formation of the Ester Linkage of the Side-Ring System During the Biosynthesis of Nosiheptide. J. Am. Chem. Soc. 139, 17438.

- (27) Yu, Y., Duan, L., Zhang, Q., Liao, R., Ding, Y., Pan, H., Wendt-Pienkowski, E., Tang, G., Shen, B., and Liu, W. (2009) Nosiheptide biosynthesis featuring a unique indole side ring formation on the characteristic thiopeptide framework. ACS Chem. Biol. 4, 855–864.
- (28) Huang, W., Xu, H., Li, Y., Zhang, F., Chen, X. Y., He, Q. L., Igarashi, Y., and Tang, G. L. (2012) Characterization of yatakemycin gene cluster revealing a radical S-adenosylmethionine dependent methyltransferase and highlighting spirocyclopropane biosynthesis. *J. Am. Chem. Soc.* 134, 8831–8840.
- (29) Watanabe, H., Tokiwano, T., and Oikawa, H. (2006) Biosynthetic study of FR-900848: origin of the aminodeoxynucleoside part. *J. Antibiot.* 59, 607–610.
- (30) Hurley, L. H., and Rokem, J. S. (1983) Biosynthesis of the antitumor antibiotic CC-1065 by Streptomyces zelensis. *J. Antibiot.* 36, 383–390.
- (31) Wang, B., LaMattina, J. W., Marshall, S. L., and Booker, S. J. (2019) Capturing Intermediates in the Reaction Catalyzed by NosN, a Class C Radical S-Adenosylmethionine Methylase Involved in the Biosynthesis of the Nosiheptide Side-Ring System. *J. Am. Chem. Soc.* 141, 5788–5797.
- (32) Zhang, Z., Mahanta, N., Hudson, G. A., Mitchell, D. A., and van der Donk, W. A. (2017) Mechanism of Class C Radical S-Adenosyl-L-methionine Thiazole Methyl Transferase. *J. Am. Chem. Soc.* 139, 18623–18631.
- (33) LaMattina, J. W., Nix, D. B., and Lanzilotta, W. N. (2016) Radical new paradigm for heme degradation in Escherichia coli O157:H7. *Proc. Natl. Acad. Sci. U. S. A. 113*, 12138–12143.
- (34) Allen, K. D., Xu, H., and White, R. H. (2014) Identification of a unique radical S-adenosylmethionine methylase likely involved in methanopterin biosynthesis in Methanocaldococcus jannaschii. *J. Bacteriol.* 196, 3315–3323.
- (35) Torres, A. G., and Payne, S. M. (1997) Haem iron-transport system in enterohaemorrhagic Escherichia coli O157:H7. *Mol. Microbiol.* 23, 825–833.
- (36) LaMattina, J. W., Delrossi, M., Uy, K. G., Keul, N. D., Nix, D. B., Neelam, A. R., and Lanzilotta, W. N. (2017) Anaerobic Heme Degradation: ChuY Is an Anaerobilin Reductase That Exhibits Kinetic Cooperativity. *Biochemistry* 56, 845–855.
- (37) Kim, H., Chaurasia, A. K., Kim, T., Choi, J., Ha, S. C., Kim, D., and Kim, K. K. (2017) Structural and functional study of ChuY from Escherichia coli strain CFT073. *Biochem. Biophys. Res. Commun.* 482, 1176–1182.
- (38) Suits, M. D., Lang, J., Pal, G. P., Couture, M., and Jia, Z. (2009) Structure and heme binding properties of Escherichia coli O157:H7 ChuX. *Protein Sci.* 18, 825–838.
- (39) Suits, M. D., Jaffer, N., and Jia, Z. (2006) Structure of the Escherichia coli O157:H7 heme oxygenase ChuS in complex with heme and enzymatic inactivation by mutation of the heme coordinating residue His-193. *J. Biol. Chem.* 281, 36776–36782.
- (40) Wyckoff, E. E., Lopreato, G. F., Tipton, K. A., and Payne, S. M. (2005) Shigella dysenteriae ShuS promotes utilization of heme as an iron source and protects against heme toxicity. *Journal of bacteriology* 187, 5658–5664.
- (41) Suits, M. D., Pal, G. P., Nakatsu, K., Matte, A., Cygler, M., and Jia, Z. (2005) Identification of an Escherichia coli O157:H7 heme oxygenase with tandem functional repeats. *Proc. Natl. Acad. Sci. U. S. A. 102*, 16955–16960.
- (42) Trott, O., and Olson, A. J. (2009) AutoDock Vina: improving the speed and accuracy of docking with a new scoring function, efficient optimization, and multithreading. *J. Comput. Chem.* 31, 455–461
- (43) Moriarty, N. W., Grosse-Kunstleve, R. W., and Adams, P. D. (2009) electronic Ligand Builder and Optimization Workbench (eLBOW): a tool for ligand coordinate and restraint generation. *Acta Crystallogr., Sect. D: Biol. Crystallogr.* 65, 1074–1080.
- (44) Gasteiger, E., Gattiker, A., Duvaud, S., Wilkins, M. R., Appel, R. D., and Bairoch, A. (2005) Protein Identification and Analysis Tools

on the ExPASy Server. In *The Proteomics Protocols Handbook*, pp 571-607.

- (45) Laue, T. M., Shah, B. D., Ridgeway, T. M., and Pelletier, S. L. (1992) in *Analytical Ultracentrifugation in Biochemistry and Polymer Science*, pp 90–125, Royal Society of Chemistry.
- (46) Schuck, P. (2003) On the analysis of protein self-association by sedimentation velocity analytical ultracentrifugation. *Anal. Biochem.* 320, 104–124.
- (47) Ortega, A., Amoros, D., and Garcia de la Torre, J. (2011) Prediction of hydrodynamic and other solution properties of rigid proteins from atomic- and residue-level models. *Biophys. J. 101*, 892–898.
- (48) Joshi, S., Fedoseyenko, D., Mahanta, N., Manion, H., Naseem, S., Dairi, T., and Begley, T. P. (2018) Novel enzymology in futalosine-dependent menaquinone biosynthesis. *Curr. Opin. Chem. Biol.* 47, 134–141.
- (49) Bhandari, D. M., Fedoseyenko, D., and Begley, T. P. (2016) Tryptophan Lyase (NosL): A cornucopia of 5'-deoxyadenosyl radical mediated transformations. *J. Am. Chem. Soc.* 138, 16184–16187.
- (50) Jin, W. B., Wu, S., Jian, X. H., Yuan, H., and Tang, G. L. (2018) A radical S-adenosyl-L-methionine enzyme and a methyltransferase catalyze cyclopropane formation in natural product biosynthesis. *Nat. Commun.* 9, 2771.
- (51) Frieden, C. (1970) Kinetic aspects of regulation of metabolic processes. The hysteretic enzyme concept. *J. Biol. Chem.* 245, 5788–5799.
- (52) Kelley, L. A., Mezulis, S., Yates, C. M., Wass, M. N., and Sternberg, M. J. (2015) The Phyre2 web portal for protein modeling, prediction and analysis. *Nat. Protoc.* 10, 845–858.
- (53) Krebs, C., Broderick, W. E., Henshaw, T. F., Broderick, J. B., and Huynh, B. H. (2002) Coordination of adenosylmethionine to a unique iron site of the [4Fe-4S] of pyruvate formate-lyase activating enzyme: a Mossbauer spectroscopic study. *J. Am. Chem. Soc.* 124, 912–913.
- (54) Sekine, Y., Tanzawa, T., Tanaka, Y., Ishimori, K., and Uchida, T. (2016) Cytoplasmic Heme-Binding Protein (HutX) from Vibrio cholerae Is an Intracellular Heme Transport Protein for the Heme-Degrading Enzyme, HutZ. *Biochemistry* 55, 884–893.
- (55) Su, T., Chi, K., Wang, K., Guo, L., and Huang, Y. (2015) Expression, purification and preliminary crystallographic analysis of a haem-utilizing protein, HutX, from Vibrio cholerae. *Acta Crystallogr., Sect. F: Struct. Biol. Commun.* 71, 141–144.
- (56) Wilks, A., and Ortiz de Montellano, P. R. (1993) Rat liver heme oxygenase. High level expression of a truncated soluble form and nature of the meso-hydroxylating species. *J. Biol. Chem.* 268, 22357—22362
- (57) Wilks, A. (2002) Heme oxygenase: evolution, structure, and mechanism. *Antioxid. Redox Signaling* 4, 603–614.
- (58) Ouellet, Y. H., Ndiaye, C. T., Gagne, S. M., Sebilo, A., Suits, M. D., Jubinville, E., Jia, Z., Ivancich, A., and Couture, M. (2016) An alternative reaction for heme degradation catalyzed by the Escherichia coli O157:H7 ChuS protein: Release of hematinic acid, tripyrrole and Fe(III). *J. Inorg. Biochem. 154*, 103–113.
- (59) Jin, W. B., Wu, S., Xu, Y. F., Yuan, H., and Tang, G. L. (2019) Recent advances in HemN-like radical S-adenosyl-l-methionine enzyme-catalyzed reactions. *Nat. Prod. Rep.*, DOI: 10.1039/C9NP00032A.
- (60) Chatterjee, A., Hazra, A. B., Abdelwahed, S., Hilmey, D. G., and Begley, T. P. (2010) A "radical dance" in thiamin biosynthesis: mechanistic analysis of the bacterial hydroxymethylpyrimidine phosphate synthase. *Angew. Chem., Int. Ed.* 49, 8653–8656.
- (61) Ji, X., Mo, T., Liu, W. Q., Ding, W., Deng, Z., and Zhang, Q. (2019) Revisiting the Mechanism of the Anaerobic Coproporphyrinogen III Oxidase HemN. *Angew. Chem., Int. Ed.* 58, 6235–6238.
- (62) Arcinas, A. J., Maiocco, S. J., Elliott, S. J., Silakov, A., and Booker, S. J. (2019) Ferredoxins as interchangeable redox components in support of MiaB, a radical S-adenosylmethionine methylthiotransferase. *Protein science: a publication of the Protein Society* 28, 267–282.

- (63) Bruender, N. A., Young, A. P., and Bandarian, V. (2015) Chemical and Biological Reduction of the Radical SAM Enzyme CPH4 Synthase. *Biochemistry* 54, 2903–2910.
- (64) Deredge, D. J., Huang, W., Hui, C., Matsumura, H., Yue, Z., Moenne-Loccoz, P., Shen, J., Wintrode, P. L., and Wilks, A. (2017) Ligand-induced allostery in the interaction of the Pseudomonas aeruginosa heme binding protein with heme oxygenase. *Proc. Natl. Acad. Sci. U. S. A.* 114, 3421–3426.
- (65) Wyckoff, E. E., Schmitt, M., Wilks, A., and Payne, S. M. (2004) HutZ is required for efficient heme utilization in Vibrio cholerae. *Journal of bacteriology* 186, 4142–4151.
- (66) Haskamp, V., Karrie, S., Mingers, T., Barthels, S., Alberge, F., Magalon, A., Muller, K., Bill, E., Lubitz, W., Kleeberg, K., Schweyen, P., Broring, M., Jahn, M., and Jahn, D. (2018) The radical SAM protein HemW is a heme chaperone. *J. Biol. Chem.* 293, 2558–2572.